Synthesis and Characterization of Lead Chevrel Phase Thin Films for Hydrodesulfurization Catalysis

Irmgard M. Schewe-Miller,[†,‡,§] Kwan Felix Koo,[†,‡] Michael Columbia,[†,‡] Fan Li,[§] and Glenn L. Schrader*[,†,‡]

Department of Chemical Engineering, Center for Interfacial Materials and Crystallization, and Ames Laboratory, USDOE, Iowa State University, Ames, Iowa

Received April 29, 1994. Revised Manuscript Received October 6, 1994[⊗]

Reactive sputtering has been used to prepare the lead Chevrel phase $PbMo_6S_8$ on several substrates. The effect of processing parameters such as H_2S flow rate, Pb sputtering current, substrate temperature, and annealing temperature were found to be very important in determining sample purity. Formation of $PbMo_6S_8$ from an as-deposited material apparently occurred at significantly lower annealing temperatures (400–800 °C), compared to conventional solid-state preparations (1000 °C). The thin films of $PbMo_6S_8$ were active thiophene hydrodesulfurization catalysts: the absence of impurities including MoS_2 could be confirmed for these materials, before and after reaction. Because the characteristic catalytic properties of the lead Chevrel phases were observed, reactive sputtering may be applicable for the preparation of other Chevrel phases on catalyst supports.

Introduction

Chevrel phases ($M_xMo_6S_8$, where M = rare earth metals, Pb, Sn, In, Ni, Co, and others) are catalysts for hydrodesulfurization (HDS) reactions.[1-6] Refining operations involving hydroprocessing are the largest-volume applications of HDS catalysis: the production of clean fuels, lubricants, and petrochemical feedstocks requires the removal of the organosulfur compounds typically found in crude oil fractions. During HDS, organosulfur compounds react with H_2 to produce sulfur-free hydrocarbons and H_2S.[7-9] The importance of hydroprocessing has continued to increase because of the use of heavier petroleum feeds.[10] Larger amounts of organosulfur compounds are present, and the reduction of the sulfur content has become more difficult to achieve. At the same time, air-quality regulations for refineries, power plants, and automobiles have become more restrictive.

Commercial hydroprocessing catalysts have typically relied on "sulfided" $CoO-MoO_3/\gamma-Al_2O_3$, $NiO-MoO_3/\gamma-Al_2O_3$, or $NiO-WO_3/\gamma-Al_2O_3$; these materials have been investigated for nearly 60 years.[11] As a result of the sulfiding conditions (either "presulfiding" by H_2S and H_2 prior to introduction of the feed or during the reactor startup), the molybdate phases undergo a transformation to a Mo sulfide phase which apparently consists of small MoS_2 crystallites with the promoters (Co or Ni) present at edges or defect sites; a "Co–Mo–S" phase has also been investigated by several groups.[12-16] The oxidation state of Mo in these materials is primarily +4, although the active sites have been proposed to be Mo^{2+} or Mo^{3+}.[17-21]

Chevrel phases ($M_xMo_6S_8$) have been referred to as reduced molybdenum sulfides because their low Mo oxidation state (relative to MoS_2). Depending on the ternary metal M and the stoichiometric coefficient x, formal oxidation states for Mo are between about +2 and $+2^2/_3$.[22-25] Our previous work has indicated that a large number of Chevrel phases are catalysts: the selectivity of Chevrel phases is remarkable since S

† Department of Chemical Engineering.
‡ Center for Interfacial Materials and Crystallization.
§ Ames Laboratory, USDOE.
* To whom correspondence should be addressed.
⊗ Abstract published in *Advance ACS Abstracts,* November 1, 1994.

(1) McCarty, K. F.; Schrader, G. L. *Ind. Eng. Chem. Prod. Res. Dev.* **1984**, *23*, 519.
(2) McCarty, K. F.; Schrader, G. L. In *Proceedings of the 8th International Congress on Catalysis*; Ertl, E. Ed.; Dechema: Berlin, 1984.
(3) McCarty, K. F.; Anderegg, J. W.; Schrader, G. L. *J. Catal.* **1985**, *93*, 375.
(4) Ekman, M. E.; Anderegg, J. W.; Schrader, G. L. *J. Catal.* **1989**, *117*, 246.
(5) Schrader, G. L.; Ekman, M. E. In *Advances in Hydrotreating Catalysts*; Occelli, M. L., Anthony, R. G. Eds.; Elsevier: Amsterdam, 1989; pp 41–66.
(6) Kareem, S. A.; Miranda, R. *J. Mol. Catal.* **1989**, *53*, 275.
(7) McCulloch, D. C. In *Applied Industrial Catalysis*; Leach, B. E., Ed.; Academic Press: New York, 1983; Vol. 1, p 70.
(8) Occelli, M. L.; Anthony, R. G. Eds. *Hydrotreating Catalysts*; Elsevier: Amsterdam, 1989.
(9) Trambouze, P. In *Chemical Reactor Technology for Environmentally Safe Reactors and Products*; de Lasa, H. I., Dogu, G., Ravella, A., Eds.; Kluwer Academic Publishers: Dordrecht, Netherlands, 1992; p 425.
(10) Beaton, W. I.; Bertolacini, R. J. *Catal. Rev.-Sci. Eng.* **1991**, *33*, 281.
(11) Prins, R.; DeBeer, V. H. J., Somorjai, G. A. *Catal. Rev.-Sci. Eng.* **1989**, *31*, 1.
(12) Topsoe, H.; Clausen, B. J. *Catal. Rev.-Sci. Eng.* **1984**, *26*, 395.
(13) Topsoe, H.; Clausen, B. J.; Topsoe, N.-Y.; Pedersen, E. *Ind. Eng. Chem. Fundam.* **1986**, *25*, 25.
(14) Ryan, R. C.; Kemp, R. A.; Smegal, J. A.; Denley, D. R.; Spinnler, G. E. In *Hydrotreating Catalysts*; Occelli, M. L., Anthony, R. G., Eds.; Elsevier: Amsterdam, 1989; p 21.
(15) Chianelli, R. R.; Ruppert, A. F.; Behal, S. K.; Kear, B. H.; Wold, A.; Kershaw, R. *J. Catal.* **1985**, *92*, 56.
(16) Roxlo, C. B.; Daage, M.; Ruppert, A. F.; Chianelli, R. R. *J. Catal.* **1986**, *100*, 176.
(17) Delvaux, G.; Grange, P.; Delmon, B. *J. Catal.* **1979**, *56*, 99.
(18) Alstrup, I.; Chorkendorff, I.; Candia, R.; Clausen, B. S.; Topsoe, H. *J. Catal.* **1982**, *77*, 397.
(19) Voorhoeve, R. J. H. *J. Catal.* **1971**, *23*, 236.
(20) Konings, A. J. A.; Valster, A.; de Beer, V. H. J.; Prins, R. *J. Catal.* **1982**, *76*, 466.
(21) Thakur, D. S.; Delmon, B. *J. Catal.* **1985**, *91*, 308.
(22) Chevrel, R.; Sergent, M. *Top. Curr. Phys.* **1982**, *34*, 25.
(23) Yvon, K. *Top. Curr. Phys.* **1982**, *34*, 87.
(24) Yvon, K. *Curr. Top. Mater. Sci.* **1979**, *3*, 53.
(25) Chevrel, R.; Hirrien, M.; Sergent, M. *Polyhedron* **1986**, *5*, 87.

0897-4756/94/2806-2327$04.50/0

removal reactions appear to be strongly favored over hydrogenation reactions.[3,26]

In our previous studies Chevrel phase catalysts were prepared by solid-state syntheses in order to ensure high-purity and rigorous control of stoichiometry. Characterization was performed before and after catalytic studies using X-ray diffraction (to examine crystallinity and phase composition), laser Raman spectroscopy (to detect impurities, including amorphous materials such as MoS_2), and X-ray photoelectron spectroscopy (to determine Mo oxidation states and surface composition). The surface areas of the catalysts prepared by the solid-state synthesis were low (0.5−2 m^2/g). This can make comparisons with other catalysts difficult if the low conversion levels result in different product distributions. Industrial applications of Chevrel phase materials will also likely require higher surface area materials.

A typical method for increasing the dispersion of catalytic materials is to use a high surface area support. For HDS catalysis, oxides such as γ-Al_2O_3 have been widely used, although the nature of molybdates on other supports has also been studied.[27] However, the formation of Chevrel phases on the surfaces of supports has not been thoroughly investigated for catalytic applications. Impurities which also are active catalysts, such as MoS_2, must be avoided. Changes in activity or selectivity due to oxidation by the support are also possible. Furthermore, despite the importance of preparing dispersed materials, characterization consequently becomes more difficult. Highly dispersed materials prepared on aluminas (surface areas of about 200−300 m^2/g) can be very difficult to characterize.

The purpose of our work has been to develop techniques for preparing Chevrel phase catalysts on supports or substrates. In this research, we have also sought to provide thorough characterization of the materials and to develop an understanding of the formation of Chevrel phase thin films. Some synthetic techniques are not readily adaptable for preparing supported phases. In our previous studies, solid-state preparation techniques were used in which stoichiometric ratios of metals and binary sulfides were ground together, pressed into pellets, sealed in evacuated fused silica tubes, and annealed at 1000−1200 °C for 1−4 days. Repetition of the grinding, pressing, and annealing procedure was sometimes required; the presence of other materials during annealing (other metal sulfides, Chevrel phases, or "oxygen-getters") was also frequently required to obtain the proper stoichiometry. Very pure, crystalline products could be obtained. Solid-state preparations with the presence of oxide supports, however, have not been reported and would probably be difficult to implement. Another potential method for dispersing Chevrel phases involves the use of thiomolybdates and salts of the ternary metal in solution.[28,29] "Precipitates" of these materials (with or without a suitable support material) were heated to temperatures of 600−1000 °C in the presence of H_2. Characterization of the resulting materials revealed the presence of a high amount of impurities, including the possible formation of MoS_2 (an active catalyst). Other severe limitations are imposed by the application of the high temperatures: a substantial reduction in surface area of the γ-alumina probably results.

In our studies of the catalytic properties of Chevrel phases on supports or substrates, we have used reactive sputtering to produce thin film materials on metal oxide and metal surfaces. This synthesis approach was selected because (1) the Chevrel phase materials can be produced in high purity, (2) extensive characterization of the thin films can be performed using key techniques, (3) the resulting materials are active and selective catalysts and their properties compare favorably with our previous results for bulk Chevrel phases, and (4) the thin-film materials are potentially more suitable for fundamental studies of catalyst−support interactions. Sputtering techniques have also been used previously to produce Chevrel phases as thin films, primarily in order to investigate superconducting properties. Our approach using reactive sputtering for catalytic applications has been unique, but this previous work has guided some aspects of our synthesis approach. Although evaporative techniques have also been used to produce thin films of Chevrel phase materials, the application of this technique for catalytic materials would probably be hindered by the necessary high temperatures and by the difficulty of controlling the stoichiometry (especially S deficiency).

Table 1 provides a summary of some of the previous research on the preparation of Chevrel phase thin films by sputtering. This summary is not intended to be exhaustive: studies have been selected which are particularly applicable to our research on catalytic materials. These studies provide detailed information on sputtering process parameters and/or include thorough characterization of the structure, composition, and purity of the thin films; in some cases, highly useful information on processing parameter "optimization" has also been provided. We have also emphasized specific Chevrel phases which in our previous research had desirable catalytic properties (high activity, selectivity, and stability).

RF sputtering was used first to prepare thin films of Cu, Ag, Pb, and Sn Chevrel phases.[30−33] Targets were constructed of pressed MoS_2 powder that had overlaying wedges of Mo metal and the ternary component (as a metal or metal sulfide, depending on the melting point of the ternary metal). Sputtering from these "composite" targets was suggested to be preferable to "homogeneous ternary sulfide" targets because it was believed that the latter would produce S-deficient films. RF sputtering was required because of the poor conductivity of MoS_2. Mo or sapphire substrates were used: in some cases, the substrates were unheated, but temperatures as high as 600−900 °C have also been employed. Films prepared at low temperature were amorphous and required annealing in sealed quartz tubes for up to 24 h with He backfilling and a small amount of the ternary metal present. This processing resembles bulk sample

(26) Sauer, N. N.; Markel, E. J.; Schrader, G. L.; Angelici, R. J. *J. Catal.* **1989**, *117*, 295.
(27) Oberlander, R. K. *Appl. Ind. Catal.* **1984**, *3*, 64.
(28) Rabiller-Baudry, M.; Chevrel, R.; Sergent, M. *J. Alloys Compd.* **1992**, *178*, 441.
(29) Rabiller-Baudry, M.; Sergent, M.; Chevrel, R.; Prouzet, E.; Dexpert, H. *Eur. J. Solid State Inorg. Chem.* **1992**, *29*, 593.
(30) Banks, C. K.; Kammerdiner, L.; Luo, H. L. *J. Solid State Chem.* **1975**, *15*, 271.
(31) Alterovitz, S. A.; Woolham, J. A.; Kammerdiner, L.; Luo, H. L. *Appl. Phys. Lett.* **1977**, *31*, 233.
(32) Alterovitz, S. A.; Woolham, J. A.; Kammerdiner, L.; Luo, H. L. *Appl. Phys. Lett.* **1978**, *33*, 264.
(33) Alterovitz, S. L.; Woolham, J. A.; Kammerdiner, L.; Luo, H. L. *J. Low Temp. Phys.* **1978**, *30*, 797.

Table 1. RF, Dc, and Reactive Sputtering of Selected Chevrel Phases

Chevrel phases	targets: composition	sputtering pressure, composition	substrate, temp	annealing conditions: temp, time, other components present	thickness	impurities, stoichiometry, microstructure	refs
			RF Sputtering:				
Cu, Ag phases	composite: MoS_2[a] Mo[b] Cu[b] or Ag[b]	1.4×10^{-2} Torr, Ar	Mo or sapphire 600–800 °C	700–1100 °C, 3–8 h (with small amount of Ag)	1–several μm	MoS_2	30, 31
Pb, Sn phases	composite: MoS_2[a] Mo[b] Sn or Pb sulfides[a]	1.4×10^{-2} Torr, Ar	Mo, unheated	1100 °C, 3–8 h (with a small amount of Pb or Sn)	1–several μm	Mo and Pb	30–33
Cu phase	composite: MoS_2[a] Mo[b] Cu[b]		sapphire 700–900 °C			Cu deficiency or Cu, Mo metal present, small grain size	32, 34
Cu phase	composite: MoS_2[a] Cu[b]		sapphire 200–400 °C 750–900 °C	900 °C, 2 h 900 °C, 24 h	3 μm	S-rich surfaces; O and C impurities; smooth, oriented films	35, 36
			Dc Sputtering				
Pb, Cu, Sn, and doped phases	mixture: MoS_2[a] PbS,[a] Cu,[a] Sn,[a] or rare earth sulfides	10^{-1} Torr, Ar	sapphire room temperature 850 °C	850–1100 °C, 1–2 h; room temperature to 1050 °C at 5 °C/min, 2 h	0.4–0.5 μm	secondary phases, MoS_2	37–41
Ho phase	$Ho_{1.25}Mo_6S_8$[c]	10^{-1} Torr, Ar	sapphire, <300 K	1200 °C, 3 h, $Ho_{1.25}Mo_6S_8$	1 μm or less	O impurities (<2% Ho_2O_2S)	42
Pb, Ba phases	$PbMo_6S_8$[c] $BaMo_6S_8$[c]	3×10^{-2} Torr, Ar	sapphire, 77–373 K	1050 °C, 3 h	0.5–2 μm	<5% Mo, Mo_2S_3	43, 44
			Reactive Sputtering				
Ag phase	Mo Ag	4.5×10^{-3} Torr, Ar, H_2S	sapphire, 800–1000 °C		0.5–1 μm	O impurities, oriented films	45–47

[a] Pressed powder. [b] Metal wedges. [c] Sintered material.

preparation: however, the films frequently also contained MoS_2. In some cases, a S deficiency affected the film composition, or the ternary metal (such as Pb) tended to evaporate.[30] For Cu phase thin films prepared on sapphire, MoS_2–Cu and MoS_2–Mo–Cu composite targets have been employed.[30–36] Microprobe analysis of the films indicated that if the deposition temperature was low (200–400 °C), excess S was present in the films. There also was evidence for O and C contamination of some films. Chevrel phases could be formed at the higher deposition temperatures, but annealing was necessary to significantly improve crystallization and growth. Smooth, oriented films could be obtained which were 1–2 μm thick. However, other studies indicated that the Cu phase films had a Cu "deficiency" for some processing parameters (although the composition of this Chevrel phase apparently may vary). Cu and Mo (up to 15%) "secondary phases" were believed to be present for other processing parameters. Superconductivity measurements indicated that the first several layers adjacent to the substrate were of inferior quality or were not superconductive at all.[33]

Dc sputtering has been used also to produce Pb, Cu, Sn, and Ho Chevrel phase films: targets were pressed powders of mixed metal sulfides and metals and were sufficiently conductive for application of this technique.[37–44] In these studies, the sapphire substrate was unheated ("room temperature") or cooled (as low as 77 K). Deposition of compounds containing Pb or Sn was believed to be especially difficult because of the potential evaporation of the elements from heated substrates. Cooling the substrates during sputtering incorporated these compounds into the amorphous deposits which subsequently were annealed. Traces of other impurities could be detected in some films, but identification by XRD was impossible because of the broad diffraction patterns. However, at least some films (for example, "$PbMo_{6+x}S_{8-y}$" samples) contained MoS_2. For other studies, Chevrel phases were used as the target materials, magnetron sputtering systems were used in some cases.[41–44] For Chevrel phases such as $HoMo_6S_8$, oxygen contamination appeared almost unavoidable since 3–4% Ho_2O_2S could be detected in the films. The possibility that the Al_2O_3 surface also contributed to the oxygen contamination was also considered. Samples prepared from the Chevrel phase targets generally have been annealed. Impurities identified by XRD for Pb and Ba Chevrel phase thin films included Mo and Mo_2S_3, although the amounts were believed to be small.[42–44]

(34) Ohtaki, R.; Zhao, B. R.; Luo, H. L.; Davis, N. M. *Mater. Res. Bull.* **1982**, *17*, 575.
(35) Ohtaki, R.; Zhao, B. R.; Luo, H. L. *J. Low Temp. Phys.* **1984**, *54*, 119.
(36) Zhao, B. R.; Ohtaki, R.; Luo, H. L., Flesner, L. D. *Thin Solid Films* **1983**, *110*, 185.
(37) Przyslupski, P.; Horyn, R.; Szymaszek, J. *Solid State Commun.* **1978**, *28*, 869.
(38) Przyslupski, P.; Horyn, R.; Gren, B. *J. Low Temp. Phys.* **1980**, *38*, 93.
(39) Przyslupski, P.; Gren, B. *J. Low Temp. Phys.* **1982**, *46*, 279.
(40) Przyslupski, P.; Poppe, U. *Solid State Commun.* **1985**, *53*, 703.
(41) Przyslupski, P.; Poppe, U.; Fischer, K.; Buchal, C. *Z. Phys. B.—Condens. Matter* **1985**, *59*, 407.
(42) Hertl, G.; Adrian, H.; Nölscher, C.; Saemann-Ischenko, G.; Söldner, L. *Physica* **1981**, *107B*, 653.
(43) Hertl, G.; Adrian, H.; Bieger, J.; Nölscher, C.; Söldner, L.; Saemann-Ischenko, G. *Phys. Rev. B* **1983**, *27*, 212.
(44) Adrian, H.; Pfirsch, F. *Phys. Rev. B* **1984**, *29*, 1447.

Most of this prior research focused on target fabrication or emphasized a two-step deposition–annealing process. Control of sample stoichiometry was difficult, and impurities or contaminants were present for many circumstances (although this did not necessarily restrict the observation of superconductivity). Reactive sputtering was used in an attempt to avoid many of these problems: in this approach, separate metal targets have been used, and a reactive gas (H_2S) was present. For some materials, direct formation of the Chevrel phase on a heated substrate was possible. A systematic study of the deposition of $AgMo_6S_8$ films demonstrated the versatility of this preparation method.[45–47] Several processing parameters strongly affected the deposition rates and the superconductivity of the films: the Mo deposition rate and the flow rate of H_2S were particularly crucial, as was the substrate temperature. The ternary metal was believed to be incorporated in the film at the appropriate stoichiometry only if Mo "sticks to the substrate" (or perhaps other sulfide precursor phases). Although XRD detected the presence of the Ag Chevrel phase, additional compositional analysis using Auger spectroscopy detected some O incorporation in films.[47] Oriented films could be prepared on sapphire and Mo substrates at 800–1000 °C (850 °C being optimal, although accurate temperature measurements were difficult).

These studies indicate that Chevrel phases can be prepared on substrates using sputtering techniques. Because of the versatility of the reactive sputtering technique and the ability to control composition, we designed a three (metal)-target chamber into which a small amount of the reactive (H_2S) gas in Ar was introduced. This sputtering system also used an inductively heated substrate holder so that in situ heating and/or annealing could be performed. The substrate holder also was rotated during deposition, enabling more uniform deposits to be obtained. On the basis of our previous studies of the HDS activity of Chevrel phases, we chose to prepare the Pb catalysts. Not only were these materials among the most active Chevrel phases, but also their stability has been confirmed in extended reactor studies.

Experimental Procedures

Reactive Sputtering System. The films described in this work were prepared in a planar magnetron sputtering system (Plasmatron, Inc.) equipped with one RF and two dc power sources (Figure 1). The stainless steel chamber (18 in. diameter) could be evacuated using a cryopump to a base pressure of 10^{-8} Torr. The chamber wall could be heated to 98 °C or cooled to 18 °C during evacuation or deposition. The RF source, operating at 13.56 MHz with 50 Ω output impedance, produced a maximum power of 500 W. The dc source, equipped with independent voltage and current control, could be operated at a maximum of 600 V and 1.5 A. The three sputtering guns were symmetrically mounted on the top of the chamber and focused on the substrate holding platform at a distance of 10 cm. Targets were 2 in. diameter and could be "presputtered" with the use of shutters. The targets were cooled during operation (NESLAB Instruments, Inc.). The substrate platform could be rotated during deposition. Substrates could be heated to 1000 °C by a 2.5 kW induction heater

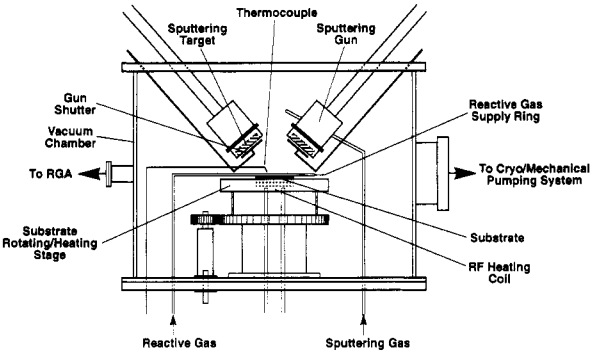

Figure 1. Schematic diagram of the sputtering system used in this work.

(Lepel Co.). A circulating water (deionized) system could be used to cool substrates.

Preparation of $PbMo_6S_8$ Thin Films. Materials were prepared from Mo (99.95%) and Pb (99.999%) targets (Superconductive Components); Ar (ultrapure carrier grade, Air Products) and H_2S (99.998%, Air Products) were used as the working and reactive gases, respectively. Sintered α-alumina plates (2 in. × 2 in., 0.025 in. thick, McMaster Carr-Supply Co.), sapphire (1 in. diameter), and Mo metal sheets (1 in. × 1 in., 0.03 in. thick) were used as substrate materials. Granules of α-alumina, produced from crushed plates and screened to 40–100 mesh, served as supports for the reactor studies. Mo metal sheets were reduced in flowing H_2 at 1000 °C for 24 h to eliminate surface oxides. Prior to deposition of the materials, all substrates were heated to 400 °C for 8 h (unless otherwise noted) under vacuum (10^{-7} Torr) to desorb surface moisture and other volatiles; the substrates then were cooled to room temperature. Representative sputtering paramaters which produced single phase films (after annealing) were: chamber pressure: 4 mTorr; Ar flow rate: 8 sccm; H_2S flow rate: 15 and 7 sccm (dependent on the "age" of the Mo target and as "optimized" over a series of depositions); Pb sputtering current 25 mA; Mo sputtering power 120 W; deposition time 30 min. For these sputtering parameters film growth rates of about 150 Å/min were observed. The films were annealed for 4 h at 800 °C in evacuated ($<10^{-5}$ Torr) fused silica tubes or within the sputtering chamber.

Characterization. The crystallinity, purity, and orientation of the deposited materials were examined by X-ray diffraction (XRD), using a Siemens D500 diffractometer (Cu Kα radiation). The crystallization process was studied using a high-temperature powder diffractometer (HTPD);[48] amorphous thin films were deposited onto Mo metal sheets (1 × 10 cm^2), and chromel–alumel thermocouples were spot welded to the backside of these Mo metal sheets. The samples were then mounted in the HTPD which is equipped with a rotating anode Cu Kα source, a multifunctional cylindrical chamber, and a gas-flow proportional position sensitive detector. The sample was heated by a current passed through the Mo metal sheets, and the temperature was controlled with a RE240O thermocontroller. The experiments were run under a dynamic vacuum of about 10^{-7} Torr or under a He gas atmosphere of about 10 Torr. The collection time for all patterns was 3 min. A Knudsen effusion cell mass loss mass spectrometer (MLMS) system was used to identify gaseous species evolving from heated samples.[49] The Knudsen effusion cell (W crucible of 1 mL volume with a 0.5 mm diameter orifice) was suspended from a microbalance, and the gaseous species were monitored using a quadrupole mass spectrometer. Evolving species could be distinguished from background species by use of a shutter between the orifice and the mass spectrometer. The temperature was measured using a thermocouple positioned near the outside of the Knudsen effusion cell which contained the sample. Laser Raman spectra (LRS) were recorded using a

(45) Hertl, G.; Orlando, T. P.; Tarascon, J. M. *Physica* **1985**, *135B*, 168.
(46) Hertl, G.; Orlando, T. P.; Tarascon, J. M. *J. Appl. Phys.* **1987**, *61*, 4829.
(47) Neal, M. J.; Orlando, T. P.; Tarascon, J. M. *Adv. Cryog. Eng.* **1988**, *34*, 689.
(48) Polonka, J.; Xu, M.; Li, Q.; Goldman, A. I.; Finnemore, D. K. *Appl. Phys. Lett.* **1991**, *59*, 3640.
(49) Schiffman, R. A.; Franzen, H. F.; Ziegler, R. J. *High Temp. Sci.* **1982**, *15*, 69.

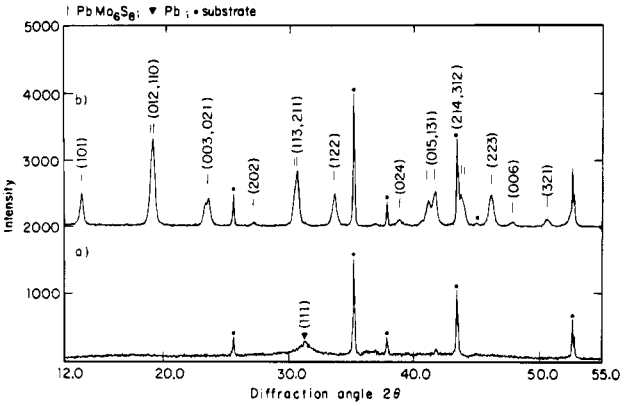

Figure 2. XRD diagrams of thin films deposited on α-Al_2O_3 plates with the optimized sputtering parameters. (a) As-deposited film, showing background scattering from an amorphous Pb–Mo–S phase and a broad (111) reflection from poorly crystallized Pb metal. (b) Single-phase $PbMo_6S_8$ film after annealing for 4 h at 800 °C in an evacuated sealed fused silica tube. The reflections are indexed according to the hexagonal setting of the rhombohedral unit cell. The labeling of the peaks is according to the following symbols: | = $PbMo_6S_8$, ▼ = Pb metal, ● = α-Al_2O_3 substrate.

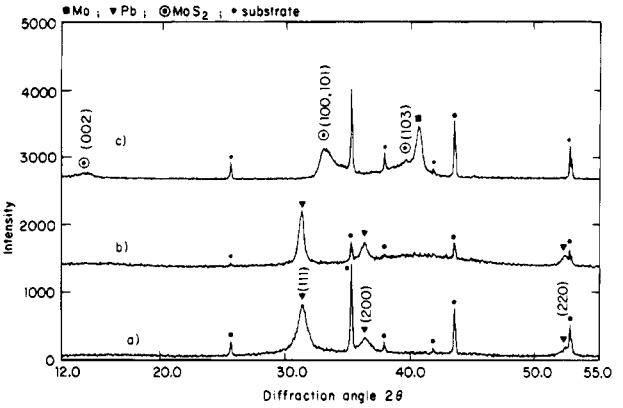

Figure 3. XRD diagrams of thin films deposited at different temperatures. (a) At about 150 °C (no heating), (b) 300 °C, and (c) 600 °C. The labeling of the peaks is according to the following symbols: ■ = Mo metal, ⊙ = MoS_2, ▼ = Pb metal, ● = α-Al_2O_3 substrate.

Spex 1877 Triplemonochromator, a Spex 164 Ar ion laser (operating at 514.4 nm and 200 mW measured at the source), and an EG&G OMAII data acquisition system. This technique was used primarily to detect amorphous MoS_2, but low levels of oxides can potentially be detected also. Scanning electron micrographs (SEM) were obtained on a JEOL JSM-840A scanning microscope to examine the microstructure of the films and substrates and to determine the thickness of the deposits. Energy-dispersive X-ray spectroscopy (EDS, Kevex Delta V microanalyzer system) was used to provide information about elemental composition. BET surface areas were determined using a Micrometrics 2100 E AccuSorb instrument. Krypton at liquid nitrogen temperatures was used as the adsorbing gas.

Activity Measurements. Thiophene (Alfa, 99%) HDS activity measurements were performed at 400 °C and about 1 atm using a continuous-flow microreactor.[50] Catalysts were heated from room temperature to 400 °C in He (19 mL/min, STP); after 1 h, the flow was replaced with a continuous flow of 2 mol % thiophene in H_2 (22 mL/min, STP). Product separation and analysis were performed by an Antek 310/40 gas chromatograph equipped with a flame ionization detector and a 12 ft *n*-octane/porasil C column. Peak intensities were integrated by a Hewlett-Packard 3390A integrator. Conversion of thiophene by the reactor (0.04%) was subtracted from the total conversion. After 10 h of continuous thiophene reaction, the reactor was purged and cooled in a stream of He, and the used catalysts were characterized.

Results

Sputtering Parameters. Figure 2 shows XRD diagrams of thin films deposited on an α-Al_2O_3 plate for the "optimized" sputtering paramaters. Figure 2a corresponds to the as-deposited film, which has background scattering from an amorphous phase and a broad (111) reflection from poorly crystallized Pb metal. After annealing for 4 h at 800 °C in an evacuated sealed fused silica tube, the characteristic reflections of a single-phase $PbMo_6S_8$ film were observed (Figure 2b). Indexing is according to the hexagonal setting of the rhombohedral unit cell of $PbMo_6S_8$.

XRD diagrams for films deposited at three different temperatures are shown in Figure 3: (a) at about 150 °C (no heating); (b) at 300 °C; (c) at 600 °C. Poorly crystalline Pb was present in the films 3a and 3b but not in 3c; MoS_2 was apparent in 3c. After samples 3a and 3b were annealed, $PbMo_6S_8$ was formed, but the film deposited without heating was more crystalline. Subsequent depositions were performed on nonheated substrates.

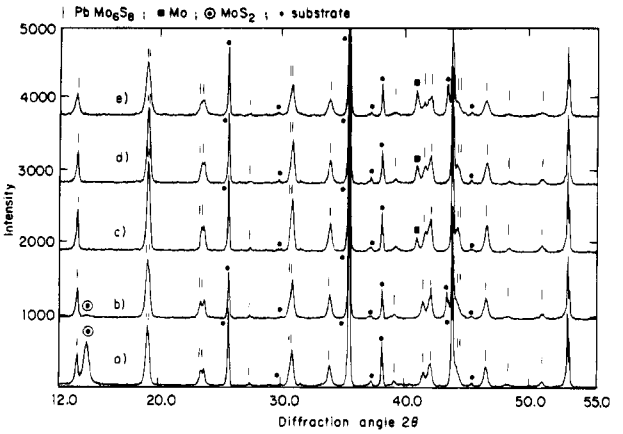

Figure 4. XRD diagrams of thin films deposited at different H_2S partial pressures, and subsequently annealed in evacuated sealed fused silica tubes. (a) 3.17 mTorr, (b) 3.00 mTorr, (c) 2.83 mTorr, (d) 2.67 mTorr, (e) 2.4 mTorr. The labeling of the peaks is according to the following symbols: | = $PbMo_6S_8$, ■ = Mo metal, ⊙ = MoS_2, ● = α-Al_2O_3 substrate.

The H_2S partial pressure was also an important deposition process parameter (Figure 4). At lower partial pressures of H_2S, Mo metal was detected after annealing in the primarily $PbMo_6S_8$ films, whereas MoS_2 was present for films prepared at higher partial pressures. $PbMo_6S_8$ was the predominant component for all annealed films: $PbMo_6S_8$ apparently can be formed over a wide range of total film composition. The Mo sputtering rate was observed to decrease gradually with the "age" of the Mo target (for an applied sputtering power), which is not uncommon in sputtering techniques. The H_2S flow rate was lowered correspondingly to obtain single phase $PbMo_6S_8$ films. An "optimal" H_2S flow rate could be reestablished by a series of depositions and comparing the diffraction patterns of the annealed films (cf. Figure 2). Since MoS_2 is a catalytically active material for HDS, its presence was to be strongly avoided. A small impurity of inactive Mo metal would be preferred, but the amount of this phase could also be minimized. LRS was used to detect amorphous MoS_2.

(50) Koo, K. F. Master Thesis, Iowa State University, Ames, IA, 1992.

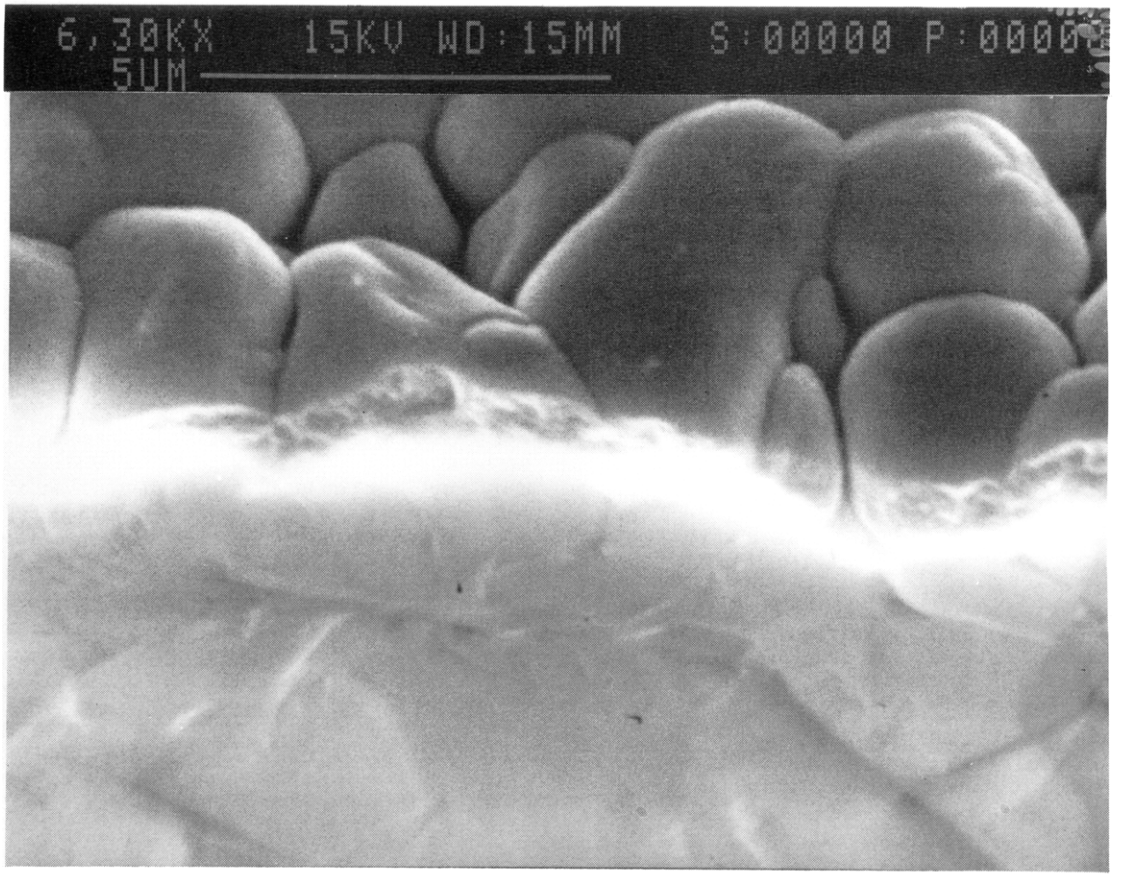

Figure 5. SEM micrograph of a freshly broken edge of an annealed $PbMo_6S_8$ film on a α-Al_2O_3 plate. Bright area, α-Al_2O_3 support; darker area, $PbMo_6S_8$ film. The film is approximately 0.5 μm thick.

The amount of crystalline Pb metal in the deposited films was determined by the Pb sputtering rate. No excess Pb was observed in annealed films with high Pb sputtering rates. On the other hand, no $PbMo_6S_8$ was formed if the Pb sputtering rate dropped below a threshold value (corresponding to about 20 mA).

Increasing the sputtering time increased the film thickness. SEM micrographs (Figure 5) revealed that the films were approximately 0.5 μm thick (30 min deposition); the growth rate of the films is therefore estimated to be about 150 Å/min. No effects of sputtering time on the film composition were observed.

Similarly no effects of using different substrate materials (α-Al_2O_3 plates, sapphire windows, Mo metal sheets) on the film composition have been detected. Therefore, different substrates were used, depending on their suitability for characterization techniques (α-Al_2O_3 for XRD and HDS reactor studies; sapphire plates for LRS; and Mo metal sheets for HTPD).

Annealing Procedure. In the earlier stages of this research, all samples were annealed in sealed evacuated fused silica tubes. The presence of additional $PbMo_6S_8$ in the same tube was found not to be necessary to produce single-phase films. However, some variation in lattice parameters of the deposited $PbMo_6S_8$ was observed. These observations followed the trends in lattice parameters observed for oxygen-for-sulfur substitutions in the structure of crystalline $PbMo_6S_8$ as reported by other authors.[51,52] To reduce exposure of the samples to air, a series of experiments was carried out in which the samples were annealed within the sputtering chamber. Formation of $PbMo_6S_8$ was observed only if a back pressure of at least 1.5 Torr of N_2 was present in the chamber. Figure 6 shows samples which were annealed at different pressures of N_2 inside the sputtering chamber. At lower pressures a broad diffraction peak near $d = 6.15$ Å indicates the formation of amorphous MoS_2 in addition to Mo metal. Single-phase $PbMo_6S_8$ thin films could still be produced from these samples if they were annealed at 800 °C in an evacuated sealed fused silica tube which also contained a small amount of Pb metal (Figure 7). If no Pb was

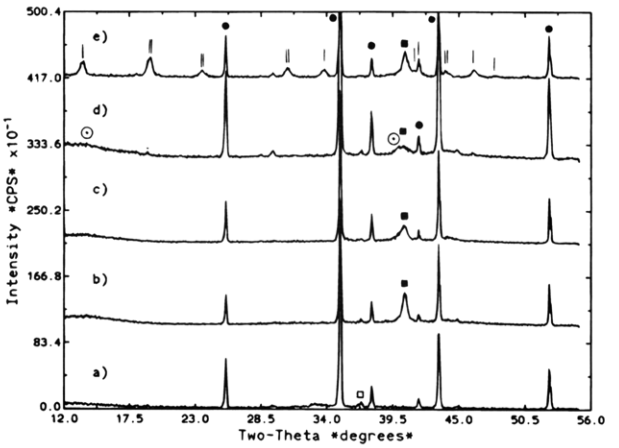

Figure 6. XRD diagrams of thin films annealed inside the sputtering chamber at different pressures of N_2: (a) as-deposited, (b) annealed in vacuum, (c) 0.08 Torr of N_2, (d) 1 Torr of N_2, (c) 1.5 Torr of N_2. The labeling of the peaks is according to the following symbols: | = $PbMo_6S_8$, ■ = Mo metal, ⊙ = MoS_2, □ = MoO_2, ● = α-Al_2O_3 substrate.

(51) Selvam, P.; Cattani, D.; Cors, J.; Decroux, M.; Niedermann, Ph.; Ritter, S.; Fischer, Ø.; Rabiller, P.; Chevrel, R.; Burel, L.; Sergent, M. *Mater. Res. Bull.* **1991**, *26*, 1151.

(52) Foner, S.; McNiff Jr., E. J.; Hinks, D. G. *Phys. Rev. B* **1985**, *31*, 6108.

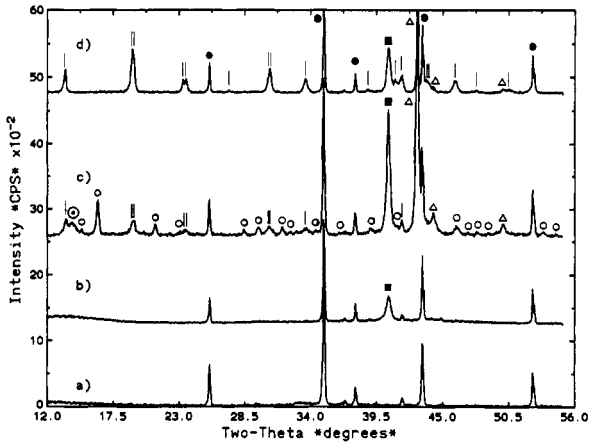

Figure 7. XRD diagrams of a thin film (a) as-deposited, (b) annealed inside the sputtering chamber in vacuum and subsequently inside an evacuated sealed fused silica tube; (c) without a piece of Pb metal, or (d) with a piece of Pb metal. The labeling of the peaks is according to the following symbols: | = $PbMo_6S_8$, ■ = Mo metal, ⊙ = MoS_2, ○ = Mo_2S_3, ● = α-Al_2O_3 substrate, △ = XRD sample holder.

Table 2. Standard Quantitative EDS Results

sample		EDS results Pb[a]	Mo	S[a]	phases detected by XRD and LRS
1	as deposited	1.4	6.0	7.9	amorphous
	annealed	0.95	6.0	7.5	$PbMo_6S_8$, little Mo metal
2	as deposited	3.5	6.0	8.9	amorphous
	annealed	1.1	6.0	11.4	$PbMo_6S_8$, little MoS_2
3	as deposited	4.4	6.0	20.3	oriented MoS_2
	annealed	(b)	6.0	12.7	oriented MoS_2

[a] Normalized to Mo = 6.0. [b] Below detection limit.

included, multiphase materials were produced with characteristic reflections for MoS_2, Mo_2S_3, Mo, and $PbMo_6S_8$.

$PbMo_6S_8$ powder (bulk) was heated up to 800 °C in a Knudsen effusion cell in the MLMS system. Evaporation of Pb was observed beginning at 550 °C which could be attributed to the sample since it was blocked by the shutter. No other observed mass peaks ($m/e \leq 300$) were suppressed by the shutter.

Table 2 shows results from standard quantitative EDS analysis of three thin-film samples before and after annealing. The surface of these samples is not smooth (cf. Figure 5), and therefore the numbers given in Table 2 have limited accuracy. Nevertheless it can be stated that the Pb content in the films decreased after annealing.

Figures 8 and 9 show sequentially recorded diffraction patterns of Pb–Mo–S thin films on Mo metal sheets which were heated in the HTPD under vacuum or under a He atmosphere, respectively. In vacuum (Figure 8) $PbMo_6S_8$ was formed at a temperature as low as 450 °C (Figure 8b,c). No changes were observed after $^1/_2$ h at 475 °C (Figure 8d), but decomposition was observed at 500 °C (Figure 8e,f). After 2 h at 500 °C the intensities of the $PbMo_6S_8$ peaks were reduced, and Mo metal and Mo_2S_3 were detected. After 4 h at 500 °C, no $PbMo_6S_8$ was present in the films. Heating the Pb–Mo–S film in about 10 Torr of He gas (Figure 9) lead to the following observations: after 45 min at 500 °C, MoO_2 and an unidentified phase were formed (Figure 9b); the unidentified phase disappeared after 1 h at 600 °C (Figure 9c). Up to this temperature no $PbMo_6S_8$ was observed. After heating the film to 640 °C the characteristic diffraction peaks of $PbMo_6S_8$ immediately appeared (Figure 9d). Further annealing at this temperature improved the crystallinity of the film slightly (Figure 9e). The formation of the MoO_2 phase was probably due to impurities in the He gas which was used without further purification. The appearance of similar peaks when the Mo metal sheets are heated under the same conditions in the HTPD confirm that assumption. The unidentified phase might also be of oxidic nature since similar very weak peaks were sometimes observed for Mo metal sheets.

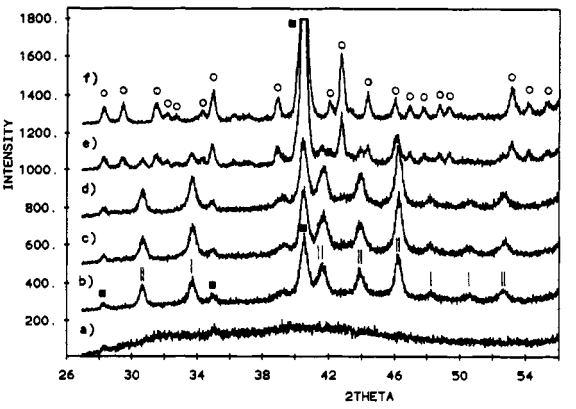

Figure 8. Sequentially recorded HTPD diagrams of a thin Pb–Mo–S film on a Mo metal substrate heated in vacuum. (a) As-deposited film at room temperature, (b) 1 h at 450 °C, (c) 3 h at 450 °C, (d) 30 min at 475 °C, (e) 2 h at 500 °C, and (f) 4 h at 500 °C. The labeling of the peaks is according to the following symbols: | = $PbMo_6S_8$, ■ = Mo metal, ○ = Mo_2S_3. Peaks of corresponding phases occur at similar 2θ values in nonlabeled patterns.

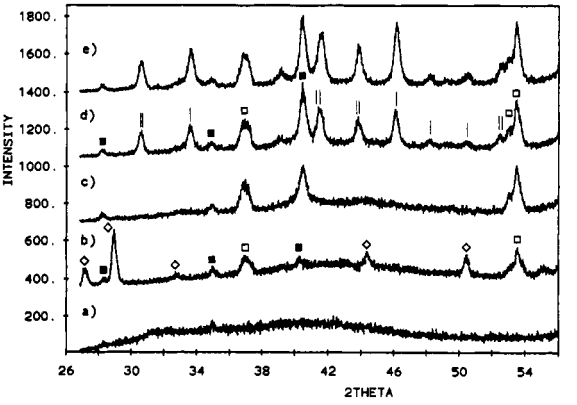

Figure 9. Sequentially recorded HTPD diagrams of a thin Pb–Mo–S film on a Mo metal substrate heated in He gas at approximately 10 Torr. (a) As-deposited film at room temperature, (b) 45 min at 500 °C, (c) 1 h at 600 °C, (d) 2 min at 640 °C, and (e) 5 h at 640 °C. The labeling of the peaks is according to the following symbols: | = $PbMo_6S_8$, ■ = Mo metal, □ = MoO_2, ◇ = unidentified phase. Peaks of corresponding phases occur at similar 2θ values in nonlabeled patterns.

Activity Measurements. $PbMo_6S_8$ deposited onto α-Al_2O_3 granules (40–100 mesh) was used to study the catalytic activity of supported Chevrel-phase materials. Tables 3 and 4 show data obtained from these materials as well as data for a bulk $PbMo_6S_8$ Chevrel catalyst and for a MoS_2-based catalyst. Although the thiophene conversion of the supported material is small due to the small surface area of the rather compact substrate material, the C_4 product distribution of the different materials shows a fairly close resemblance between the products for catalysis by bulk $PbMo_6S_8$ and thin film $PbMo_6S_8$ material. Due to the rough surface of the

Table 3. Thiophene HDS Conversion at 400 °C

catalyst	reaction time	thiophene conversion (%)	HDS rate (mol/s m^2)
$PbMo_6S_8$ on	20 min	0.691	19.50
α-Al_2O_3 granules	1 h	0.582	16.42
	10 h	0.339	9.56
$PbMo_6S_8$	20 min	1.59	4.53
	10 h	1.16	2.61
$Co_{0.25}$–Mo–S[a]	20 min	1.94	7.37
	10 h	0.77	2.92
1000 °C MoS_2[a]	20 min	2.22	2.67
	10 h	0.76	0.92

[a] Reference 5.

Table 4. C_4 Products for Thiophene HDS at 400 °C

		C_4 product distribution			
catalyst	reaction time	*n*-butane	1-butene	*trans*-2-butene	*cis*-2-butene
$PbMo_6S_8$ on	20 min	*a*	38.3	35.8	25.9
α-Al_2O_3	1 h	*a*	62.6	15.1	22.3
granules	10 h	*a*	66.3	18.5	15.2
$PbMo_6S_8$	20 min	*a*	65.5	20.2	14.3
	10 h	*a*	65.6	21.8	12.6
$Co_{0.25}$–Mo–S[b]	20 min	1.3	35.9	28.0	24.8
	10 h	1.5	36.4	41.1	21.0
1000 °C MoS_2[b]	20 min	2.67	41.2	32.7	23.7
	10 h	0.92	46.0	34.9	17.3

[a] Below detection limit. [b] Reference 5.

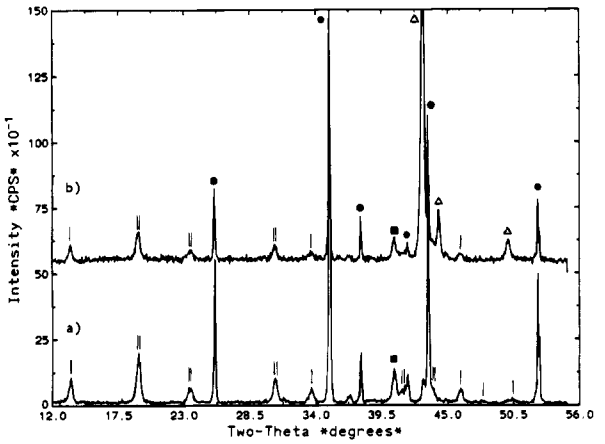

Figure 10. XRD diagrams of a thin film of $PbMo_6S_8$ on an α-Al_2O_3 plate (a) before and (b) after being exposed to the HDS reactor conditions for 10 h. The labeling of the peaks is according to the following symbols: | = $PbMo_6S_8$, ■ = Mo metal, ● = α-Al_2O_3 substrate, △ = XRD sample holder. The strong diffraction peaks arising from the XRD sample holder are due to the small sample size.

supported catalyst on the granular material no satisfactory XRD diagrams could be recorded. However, Figure 10 shows therefore the XRD patterns of a thin film of $PbMo_6S_8$ deposited on an α-Al_2O_3 plate before and after HDS reactor studies (10 h). After 10 h of HDS, the intensities of the XRD peaks decreased and the background noise increased. Some of these changes might be due to a smaller area being exposed to the X-ray beam, as indicated by the strong peaks arising from the XRD sample holder. (The dimensions of the HDS reactor allows the insertion of 2 × 15 mm^2 pieces, but the X-ray beam actually includes an area of about 10 × 30 mm^2.) It is, however, clear that the $PbMo_6S_8$ phase is still present, and formation of a new phase is not observed. The Pb Chevrel phase was chosen, in part, because of our previous work with bulk materials which indicated little surface compositional change after HDS catalysis. Although some "small cation" Chevrel phases do show surface migration of the ternary metal, "large cation" materials do not.[1-5]

Discussion

Reactive sputtering of thin films is a rather complex process which is not yet fully understood in detail for many systems. The properties of the resulting materials depend on a variety of experimental parameters, such as total pressure, sputtering power (RF sources) or current (dc sources), flow rates of the gases, substrate temperature, sputtering time, pretreatment of substrates, and the chemical nature of the substrate material itself. These experimental parameters can be translated to a certain extent into parameters like sputtering rates for the different metals and the vapor pressures for the reactive gases. The sputtering rates and the vapor pressure of the reactive gas will naturally determine the composition in the deposited film. The sputtering rate depends on several experimental parameters (total pressure, gas composition, power/current at the source, age of target, substrate temperature, and ability of the substrate to "retain" the deposited material). Simultaneous sputtering from two sources can also affect sputtering rates. The observed influences these experimental parameters have on the properties of the deposited films establish some clear trends which can now be discussed.

We have found the H_2S flow rate, and thus the H_2S partial pressure, to be the most important parameter determining the final composition of the annealed films. Since the Mo-sputtering power was constant for all experiments, this parameter directly influenced the Mo/S ratio in the deposited amorphous films. As mentioned before, the Mo sputtering rate did change slightly with the age of the target at a constant sputtering power; thus the optimal H_2S flow rate needed to be adjusted accordingly. The Mo/S ratio in the deposited films primarily determined the nature of the secondary phase (Mo or MoS_2) formed ($PbMo_6S_8$ was observed for a range of conditions). If the H_2S flow rate was excessive, $PbMo_6S_8$ was no longer present, and MoS_2 was formed when the films were annealed.

The Pb sputtering current was the next most important experimental parameter determining the properties of the films. We determined a lower threshold value of about 20 mA below which no $PbMo_6S_8$ phase formation was observed in the annealed films. Raising the Pb sputtering current to much higher values like 75 mA or greater lead to the formation of excess amounts of poorly crystalline Pb metal in the as-deposited films. However, no effect on the composition of the annealed films was observed. XRD diagrams of as deposited films differ substantially, if, under otherwise similar conditions, Pb and Mo are cosputtered, or only Pb, or only Mo are sputtered. As shown in Figure 11, the formation of crystalline PbS is suppressed by the cosputtering of Pb and Mo in an Ar/H_2S gas mixture. The intense background scattering in Figure 11a indicates the formation of an amorphous Pb–Mo–S phase instead, which seems to be a excellent precursor for the formation of the crystalline $PbMo_6S_8$ phase.

The substrate temperature is crucial, due to the low melting point and the high vapor pressure of Pb metal. Incorporation of Pb into the as-deposited films was only possible at substrate temperatures at and below 300 °C. Since the formation and crystallization of the $PbMo_6S_8$

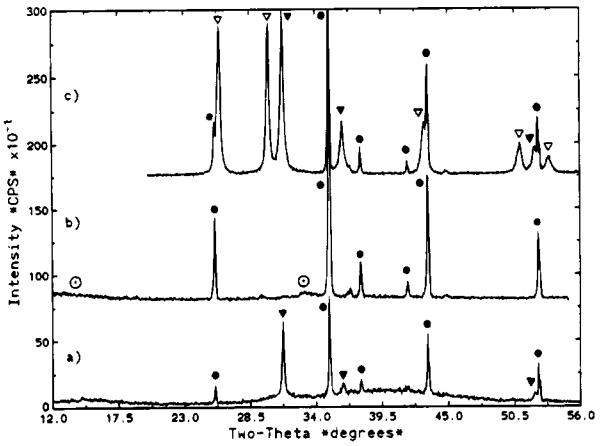

Figure 11. XRD diagrams of as-deposited thin films: (a) simultaneous sputtering of Mo and Pb, (b) sputtering of Mo only, and (c) sputtering of Pb only in and H_2S/Ar atmosphere under otherwise similar conditions. The labeling of the peaks is according to the following symbols: ▼ = Pb metal, ▽ = PbS, ⊙ = MoS_2, ● = α-Al_2O_3 substrate.

phase requires temperatures of at least 450–500 °C (under the most favorable conditions reported in our previous work[53]) or more generally at 700–800 °C, it appears to be very difficult to deposit crystalline $PbMo_6S_8$ thin films in a one-step process.

The annealing process is therefore another important experimental step in the formation of crystalline $PbMo_6S_8$ materials. The Knudsen effusion cell experiment has shown that only Pb is detected as a vapor over bulk $PbMo_6S_8$ powder in vacuum for temperatures between 550 and 800 °C. In addition we observed a reduction of the Pb content in the thin films after annealing (cf. Table 2). This helps to explain why formation of crystalline $PbMo_6S_8$ is possible when the amorphous films are annealed in evacuated sealed tubes but not in a dynamic vaccum. The small volume of the sealed tubes allows the buildup of an equilibrium Pb metal vapor pressure, and no significant losses of Pb from the films will occur in the closed system. On the other hand heating the film in a dynamic vacuum (open system) leads to a continuous removal of Pb from the films which are soon sufficiently Pb deficient that the crystalline $PbMo_6S_8$ phase cannot be formed. If these films are annealed inside evacuated sealed tubes containing a piece of Pb metal, a sufficient Pb vapor pressure is established, and $PbMo_6S_8$ can be formed (Figure 7). The evaporation of Pb metal apparently can be suppressed by the application of a backpressure of N_2 or He gas (Figures 6 and 9) in the closed sputtering chamber or the HTPD chamber, respectively.

The formation of crystalline $PbMo_6S_8$ in the dynamically evacuated HTPD-chamber at a temperature as low as 450 °C was surprising. At this temperature no detectable Pb vapor pressure was observed in the Knudsen effusion cell experiment although this temperature exceeds the melting point of Pb by about 125 °C. Some mobility of the Pb atoms can therefore be assumed which would assist the formation of crystalline $PbMo_6S_8$. Since the Pb vapor pressure is sufficiently low (1.5×10^{-12} Torr over Pb metal at 700 K[54]), no substantial evaporation of Pb will occur. The situation changes drastically when the temperature reaches 500 °C and the decomposition of $PbMo_6S_8$ is observed.

Application of a backpressure of 10 Torr of He raises the crystallization temperature to 640 °C in otherwise similar films. We suggest that the presence of a gas at low pressure in the (annealing) chamber leads to effective heat transfer between the film and the chamber; thus, the film surface is cooled and the evaporation of Pb metal is suppressed. In addition, it is likely that a strong temperature gradient across the thin film–substrate material is established. The actual temperature inside the thin film might therefore be below the temperature measured by the thermocouple (spotwelded to the backside of the substrate).

Conclusion

In all experiments a relatively fast (2 min to 4 h) formation of $PbMo_6S_8$ was observed at temperatures from 450 to 800 °C. This is well below the temperatures used in solid-state synthesis of bulk $PbMo_6S_8$ from PbS, Mo and MoS_2 (1–4 days, 1000–1200 °C). For solid-state reactions the rate of phase formation and crystallization is related to diffusion processes within grains and across grain boundaries. The formation of thin films containing an amorphous Pb–Mo–S precursor phase by reactive sputtering leads to the shortening of diffusion paths (reduction of diffusion barriers) within the films, and therefore the formation and crystallization of $PbMo_6S_8$ is accelerated.

The use of a reactive sputtering system with independently controllable sputtering guns for the different metals, and an adjustable H_2S vapor pressure also allows the film composition to be controlled. The formation of undesired components, such as the catalytically active phase MoS_2, can be effectively suppressed. The $PbMo_6S_8$ thin films supported on α-Al_2O_3 granules were active for thiophene HDS catalysis and were stable under reaction conditions based on the X-ray diffraction data obtained. Future work on the preparation of thin-film Chevrel phase materials on supports will provide more information concerning potential catalytic applications.

Acknowledgment. This work was funded by the Center for Interfacial Materials and Crystallization and the Center for Advanced Technology Development at Iowa State University. Studies involving the high-temperature X-ray diffraction were performed in the Ames Laboratory which is operated for the U.S. Department of Energy by Iowa State University under Contract No. W-7405-ENG-82, supported by the Office of Basic Energy Sciences.

(53) Schewe-Miller, I.; Li, F.; Columbia, M.; Schrader, G. L.; Franzen, H. F. *J. Alloys Comp.* **1994**, *204*, L13.

(54) Hultgren, R., Desai, P. D., Hawkins, D. T., Gleiser, M., Kelley, K. K., Wagman, D. D., Eds. *Selected Values of the Thermodynamic Properties of the Elements*; American Society for Metals: Metals Park, OH, 1973.